Prediction of Moisture Loss in Withering Process of Tea Manufacturing Using Artificial Neural Network

Nipan Das, Kunjalata Kalita, P K Boruah, and Utpal Sarma, *Member, IEEE*

***Abstract*— The first and foremost process in tea manufacturing, withering, is the foundation for producing good quality. Moisture plays an important role in the manufacturing process of tea to get the desired quality. In this paper, a novel in situ instrumentation technique is proposed and validated experimentally for prediction of moisture loss (ML) in the withering process. In the proposed technique, ML is predicted based on the inlet and the outlet relative humidity (RH) and temperature during the process of withering. Network capable smart sensor nodes are developed for the measurement of RH and temperature at the inlet and outlet of the withering trough. Architecture of the nodes and network is described. A scaled-down prototype of an enclosed trough is developed to perform withering of tea leaves. Based on the data measured by the system, ML is predicted by using artificial neural network. Nonlinear autoregressive model with exogenous inputs is used for predicting the ML. The predicted ML is compared with the actual amount of ML measured by weight loss. A total of nine experiments are conducted for nine batches of tea leaves. The data collection, their analysis and results are reported in this paper. The observed result shows a good agreement between the predicted and actual ML. The maximum mean error in prediction is −3.6%.**

***Index Terms*— Artificial neural network (ANN), humidity measurement, moisture, moisture measurement, temperature measurement.**

I. Introduction

TEA is one of the most popular beverages in the world [1], [2]. Different types of tea have different physical appearances and quality attributes which involve different kinds of processing methods [3]. Based on the variations in processing steps involved in tea manufacturing, tea can be classified into six different types, viz. green tea, yellow tea, white tea, *Oolong* tea, black tea, and postfermented tea [4]. The process "withering" is common for the manufacture of all types of tea except green and yellow tea. Withering, the first step of processing is the foundation for achieving good quality in produced tea. In withering, both physical and chemical processes are involved in which freshly plucked leaf is conditioned physically, as well as, chemically for subsequent processing stages. The physical withering reduces the moisture content (MC) of the fresh leaf which is expressed in percentage. Percentage of wither is defined as the weight in kilogram to which 100 kg of leaf is reduced at the end of the withering [5]. Moisture from the fresh tea leaves is reduced in a controlled manner so that the withering of tea leaves reaches a level of 74%–83% within the time required for chemical wither to complete which is normally about 12 to 16 h. Correct level of withering is essential for quality of produced tea, although, it has always been a difficult task to determine the endpoint of withers. Physical withering also makes the leaf "flaccid" or "rubbery" which is essential for the subsequent steps of processing [5].

Chemical withering starts immediately after plucking of tea leaves. It involves several chemical processes like release of carbon dioxide and water due to break down of larger molecules. The process also involves changes in enzyme activity and partial break down of proteins to amino acids which act as precursors for aroma and increase in caffeine content. This contributes toward briskness and production of volatile flavor components. Some of these compounds contribute to the grassy odour and others are responsible for the flowery aroma and reduction in chlorophyll content. The mentioned chemical changes are all intrinsic to the biochemical structure of the leaf, but the range and the extent of the reactions depend on the breed commonly known as *jat*, cultural practices and physical parameters like temperature and humidity. The chemical changes also contribute to the quality attributes of tea like the "body" and the "flavour" [5].

The quality of the final product is highly influenced by the withering process. Influence of withering, including leaf handling, on the manufacturing and the resulting quality of black tea was reported [6]. The duration of withering plays a vital role which contributes to some biochemical properties and sensory quality attributes of the final product. Chemical wither for longer period produces liquor with better flavor and fuller cup characters [7]. Various biochemical processes take place during withering of black tea production. The characteristics of phenol oxidase, i.e., the main enzyme of tea production and its hydroxylase and catechol oxidase activities are responsible for the main transformation of phenol compounds determining the quality of the product. Modified technologies excluding withering cannot provide high quality product [8].

Due to various advantages such as controlling the withering speed or making uniform withering by controlling speed and its direction of airflow, trough withering is widely used all

Manuscript received April 30, 2017; revised August 16, 2017; accepted August 21, 2017. The Associate Editor coordinating the review process was Dr. Anirban Mukherjee. *(Corresponding author: Nipan Das.)*

The authors are with the Department of Instrumentation and USIC, Gauhati University, Guwahati 781014, India (e-mail: nipan.das86@yahoo.co.in).

Color versions of one or more of the figures in this paper are available online at http://ieeexplore.ieee.org.

Digital Object Identifier 10.1109/TIM.2017.2754818

over the world. The troughs are of two types—(a) open trough and (b) enclosed trough [9]. However, attempts are going on for the improvement of troughs such as the one reported in [10], where withering was completed within 6 h. But it affects the biochemical pathway.

Since withering plays an important role in the final product, various attempts have been made to measure the percentage of wither using different techniques. In one such technique, the weight loss method is used where a representative section of the withering trough was used for the measurement [11]. In another method, the measurement of MC in tea is performed by the microwave transmission technique. The change in ratio of amplitude and phase shift determines the MC [12]. The capacitive fringe-field method is also used for the detection of MC of tea leaves at its final stage [13]. Drying rate is an important factor in estimating the withering of tea leaves. Drying curves of withering thin layer are reported [14], but the effect of relative humidity (RH) was unreported in the experiment. RH has a major role on withering of tea leaves [15]. A method to use temperature and humidity sensor for determining MC of *Oolong* tea by equilibrium RH and equilibrium MC was reported [16]. The techniques that are discussed have difficulties in online and *in situ* applicability in withering. Moreover, in all the approaches mentioned above, a representative sample from the trough or the process was selected for the measurement instead of considering the whole trough.

Because of the complex mechanism of moisture release by tea leaves and the use of large area troughs for withering, it is very difficult to predict the ML in withering. Level of withering is basically determined by human experts. To investigate the *in situ* and online feasibility and applicability for measuring ML in withering of tea, an instrumentation technique is proposed in which no representative sample is necessary, instead the whole trough is under consideration without any major modification of existing troughs of enclosed type. A scaled-down prototype of enclosed type trough is developed and two sensor nodes, each node consisting of a temperature sensor and an RH sensor, are installed to measure the temperature and the RH. Sensor nodes are placed at the inlet and the outlet of the air flow path of the trough. A load cell with proper signal conditioning and mechanical arrangement is also installed to obtain the weight loss of the tea leaves during withering.

In withering, the moisture removal process is accomplished by vaporizing the water contained in the tea leaves; and to do this the latent heat of vaporization must be supplied. There are two important process-controlling factors: transfer of heat to provide the necessary latent heat of vaporization and movement of water or water vapours through the tea leaves to separate the moisture.

The necessary latent heat of evaporation is achieved from the inlet temperature of the incoming air. The moving air carries evaporated water vapour toward the outlet of withering trough which raises the level of RH at the outlet compared to that at the inlet.

Moisture release from the leaves starts from the surface and later on is governed by diffusion or capillary movement [17]. Withering is a complex process, in which the release of moisture from the leaf is governed by many factors involving complicated mechanisms. Effects of temperature, RH, and air speed are more significant compared to other factors.

Since ML in withering process is highly nonlinear, ordinary statistical methods are not suitable for predicting ML. As a tool for prediction, ANN works well where other methods do not, and have been applied in solving a wide variety of problems that are not well suited for classical methods of analysis. ANN is a data-driven model [18] and it can be used in extremely complex nonlinear problems [19]. Due to the ability of realization for complex nonlinear mapping of multidimensional interrelated input and output parameters ANN provides excellent prediction model compared to expert systems or its statistical counterpart [20]. Different structures of ANNs are used depending on the type of application requirements including the food and agriculture industry [21], [22]. Application of ANN in prediction or forecasting of time series is broadly presented in [23]–[27]. For nonlinear system identification or modeling, the nonlinear autoregressive models with exogenous input (NARX) network is mostly used [28], which is computationally equivalent to Turing Machines [29], due to its capability of dynamic modeling [27]. Its applications in various modeling problems are available in [27] and [29].

Withering of tea leaf is a dynamic process and ML at a particular instant depends upon the amount of ML in its previous instants. Due to its suitability in modeling dynamic nonlinear systems and specially time series, NARX network is adopted for predicting the ML in withering process of tea. Difference of RH in the outlet and inlet, the inlet temperature and time are considered as the predictor for determining the ML (which is the response) in the withering process. Predicted amount of ML is compared with the actual amount measured by weight loss.

II. Scaled-Down Prototype of Enclosed Trough

A scaled-down prototype of enclosed type withering trough is designed with dimension (30 cm $\times$ 19 cm $\times$ 14 cm) as shown in Fig. 1(a). The bed of the trough for loading tea leaves is made of a plastic net of 5-mm grid size and is placed on top of a load cell arrangement to measure the weight loss of loaded leaves during withering. To avoid errors in the measurement of weight, a small container of PVC is attached to the net so that the loaded leaves do not come into contact with the side walls of the trough. To maximize the passage of air through the loaded leaves, the container is surrounded by aluminum sheet. A fan is attached to the trough so that air flows through circular holes (3-cm diameter) at the inlet and the outlet. To measure temperature and RH both at the inlet and the outlet, two sensor nodes are attached. One at the inlet and the other one at the outlet. The photograph of the experimental setup is shown in Fig. 1(b).

III. Instrumentation System

The instrumentation system consists of sensors, data acquisition, and logging. The sensing parameters are temperature, RH, and weight of loaded leaves. Two sensor nodes capable of measuring RH and temperature are incorporated in the

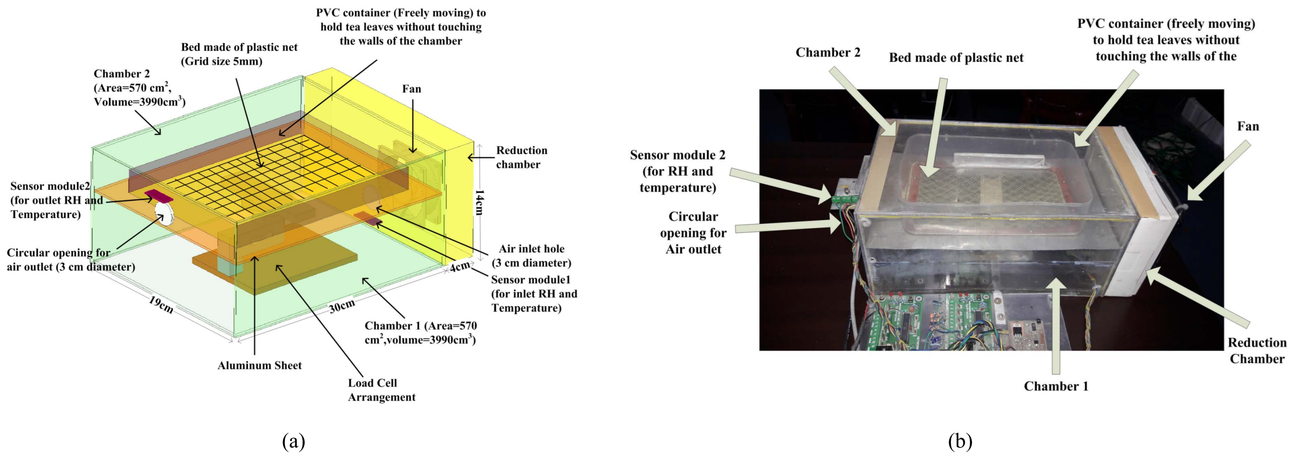

Fig. 1. (a) Prototype of enclosed withering trough showing different parts. (b) Photograph of the prototype.

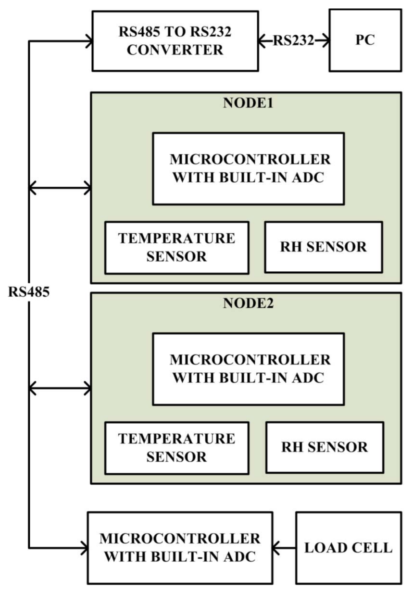

Fig. 2. Block diagram of withering trough instrumentation.

system to measure temperature and RH at the inlet and the outlet of the air flow path. A load cell, with associated signal conditioning circuits, is used to measure the weight of loaded leaves in the trough. Two microcontrollers with built-in 10-bit analog-to-digital converter (ADC) are used to read the voltage output of the sensors. The system is connected to a personal computer (PC) by RS485 communication to facilitate for data logging. The block diagram of the system is shown in Fig. 2.

A. Sensor Node

The sensors used in the node are LM35C [31] for measuring temperature and HIH5030 [32] for RH. The output of HIH5030 is dependent on the supply voltage. To get a stable supply voltage, a reference voltage generator MCP1541 [33] along with buffer made of TLC272 [34] operational amplifier is used. The accuracy of the temperature sensor, LM35C, is ±1.5 °C and its operating range is −55 °C to +150 °C. The operating range of RH sensor, HIH5030, is 0% RH to 100% RH within the temperature range of −40 °C to +85 °C. The accuracy of RH measurement is ±3% in the operating range

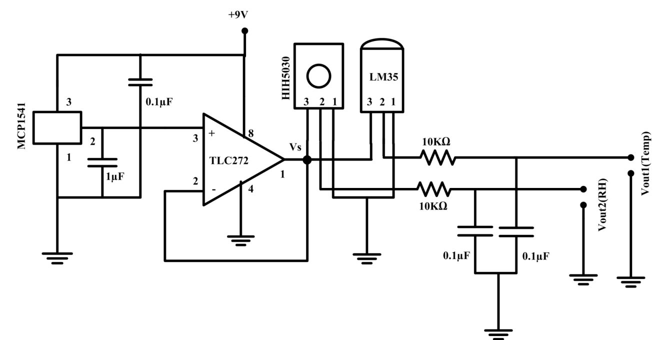

Fig. 3. Circuit schematic of sensors in node.

of 11% RH to 89% RH, whereas ±7% in the range of 0% RH to 10% RH and 90% RH to 100% RH. The circuit schematic of sensors in the node is shown in Fig. 3.

The output voltage V_{out2} (RH) (Fig. 3) and RH is related by the following equation at 25 °C [32]:

$$\text{RH} = \frac{\frac{V_{\text{out2}}(\text{RH})}{V_s} - 0.1515}{0.00636}. \quad (1)$$

The true RH requires temperature correction and is given by the following [32]:

$$\text{True RH} = \frac{\text{RH}}{(1.0546 - 0.00216T)}\% \quad (2)$$

where T is the measured temperature in degree Celsius.

The RH sensor and the temperature sensor are assembled close to each other to minimize the temperature gradient between them.

B. Load Cell Signal Conditioning and Weighing Arrangement

The signal conditioning circuit for the load cell (full bridge) is shown in Fig. 4. The circuit composed of LM336-2.5N [35] precision shunt diode, TLC272 dual operational amplifier, and AD620 [36] instrumentation amplifier. The load cell is excited by 2.5 V. The excitation voltage is obtained from a shunt regulator diode, LM336-2.5. The TLC272, precision dual operational amplifier is configured as unity gain amplifier to drive the load cell.

This article has been accepted for inclusion in a future issue of this journal. Content is final as presented, with the exception of pagination.

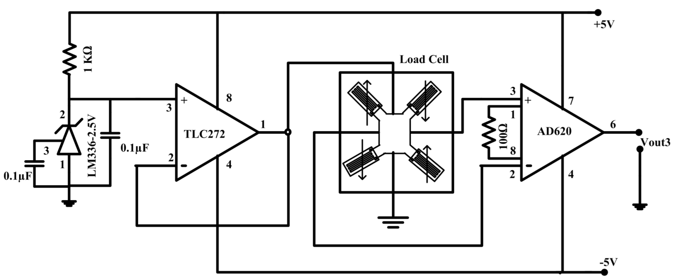

Fig. 4. Signal conditioning circuit for load cell.

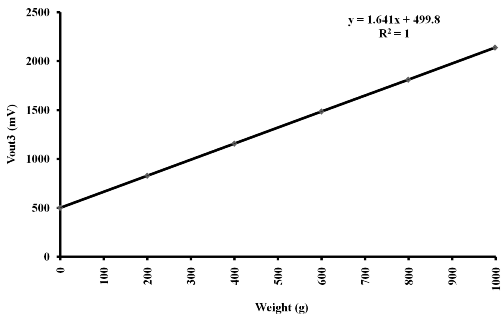

Fig. 5. Calibration of weighing system.

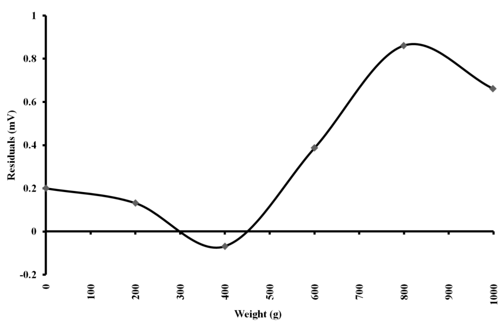

Fig. 6. Residual versus independent plot for weighing system calibration.

The shunt regulator diode, LM336-2.5, gives 2.5 V within the temperature range of 0 °C to 70 °C with 0.2-Ω dynamic impedance. The bridge output is amplified by an instrumentation amplifier, AD620, where the voltage gain is set to 495 using a 100-Ω precession resistor of 0.1% tolerance and temperature coefficient ±5 ppm. The gain equation is [36]

$$G = \frac{49.4\ \mathrm{K\Omega}}{R_g} + 1 \tag{3}$$

where G is the gain of the amplifier and R_g is the gain setting resistor.

The system is calibrated by known loads. The output (V_{out3}) for different loads are measured using a 6(1/2) digit digital multimeter (Agilent, model no: 34401A) and recorded. Using the data obtained for various loads, a calibration curve is obtained and is shown in Fig. 5.

The linear fit calibration equation is

$$y = 1.641x + 499.8 \tag{4}$$

where y is the output voltage of the weighing system in millivolt and x is the applied load in grams.

The sensitivity of the system is 1.641 mV/g. The residual versus independent plot is shown in Fig. 6.

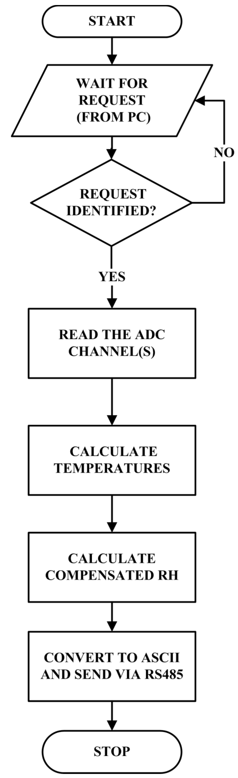

Fig. 7. Flowchart for the implemented algorithm in microcontroller.

IV. Data Acquisition System

In a sensor node, the outputs of sensors are connected to two channels of built-in 10-bit ADC of an ATmega8 [37] microcontroller. There are two such nodes in the system, which are used for measuring RH and temperature. The output voltage (V_{out3}) from the signal conditioning circuit of the load cell is connected to one 10-bit ADC channel of another ATmega8 microcontroller. The microcontrollers are connected to a PC by RS485 network. An algorithm is developed for reading the output voltages of sensors, compensating the effect of temperature in RH measurement and finally sending the data to PC in proper format. The developed algorithm is implemented in ATmega8 microcontroller by writing suitable C-code in Atmel Studio4 integrated development environment [38]. The temperature compensation is done using (1) and (2). To log the received data in a PC, a program is written in C language. Data is stored in PC in. XLS format along with records of date and time. Figs. 7 and 8 show the flowchart of developed algorithms that are implemented in the microcontroller and the PC, respectively.

V. Nonlinear Autoregressive Model With Exogenous Inputs

ANN has proved to be a very powerful tool for performing predictions and forecasts due to their prominent advantages for approximating nonlinear function and data-driven capability of forecasting and prediction [19], [20]. ANN architectures are widely classified as feed forward networks (FFN) and recurrent neural networks (RNN). In FFN, information flows only in one direction, from the input layer via some hidden

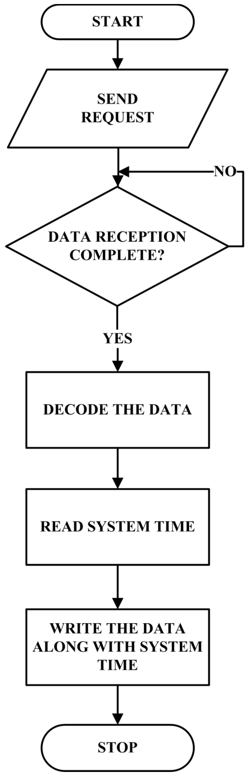

Fig. 8. Flowchart for the implemented algorithm in PC.

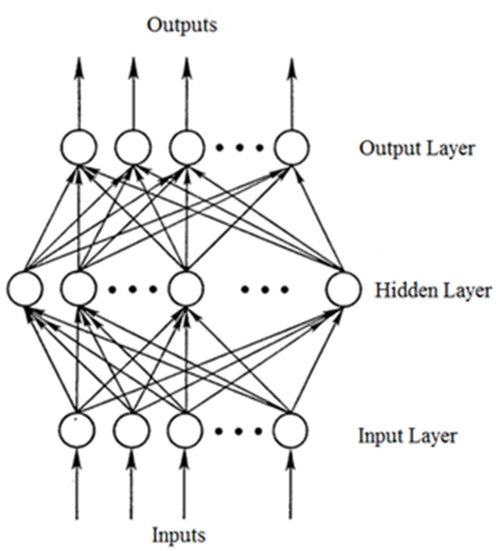

Fig. 9. Feed forward network.

layers to the output layer. Since there is no feedback (loop), output of any layer does not affect the same or preceding layer (see Fig. 9). RNN are different from FFN in the sense that these networks contain at least one feedback loop from any layer, which may also be a self-loop (see Fig. 10).

FFN networks are appropriate for any functional mapping problem where a set of responses or output variables are affected by a set of predictors or input variables.

In the RNN computations derived from earlier input are fed back into the network, which comprises memory in the network. Feedback networks are dynamic i.e., their "state"

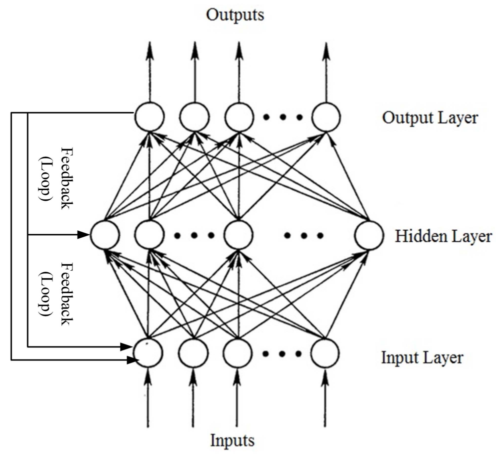

Fig. 10. Recurrent neural network.

changes in every iteration until they get a stable state. When input changes a new stable state needs to be established. RNN are suitable for modeling or predicting one or more outputs (or response of processes) in which output (or response) changes dynamically or the value of outputs (or responses) are dependent on earlier state(s) of both inputs or predictors and outputs (or responses).

NARX [28], [30] is an important class of recurrent nonlinear dynamic network, with feedback connections enclosing several layers of the network that can be mathematically represented as [28]

$$y(n+1) = f[(y(n), y(n-1), \ldots, y(n-d_y+1)); \\ (u(n), u(n-1), \ldots, u(n-d_u+1))] \quad (5)$$

where, $u(n) \in R$ and $y(n) \in R$ denote, respectively, the input and the output of the model at discrete time step n, while $d_u \geq 1$ and $d_y \geq 1$, $d_u \leq d_y$, are the input-memory and the output-memory orders. In a compact vector form, (4) can be represented as [28]

$$y(n+1) = f[y(n); u(n)] \quad (6)$$

where the vectors $y(n)$ and $u(n)$ denote the output and input regressors, respectively.

The nonlinear mapping $f(.)$ is generally unknown and can be approximated, for example, by a standard multilayer perceptron network. The resulting connectionist architecture is then called a NARX network [29], [38], [39].

NARX has two architectures: series-parallel (SP) and parallel (P). In SP mode, the output's regressor is formed only by actual values of the system's output. In case of P mode, estimated outputs are fed back and included in the output's regressor [27], [39].

Since the true output is available during the training of the network, SP architecture is used in which the true output is used instead of feedback from the estimated output, as shown in Fig. 11. Two advantages for doing this are: 1) the input to the FFN is more accurate and 2) the resulting network has a purely feed forward architecture, and static back propagation can be used for training.

TABLE I
CONFIGURATION OF NARX NETWORK

Layers	Memory/ Delay (in seconds)	Nodes	Activation function	Training Algorithm	Minimum gradient	Goal/Performance (Mean Squared Error)
Input/hidden layer	840	20	log-sigmoid	Levenberg-Marquardt backpropagation	0.00001	0.001
Output layer	1400	1	Purely Linear			

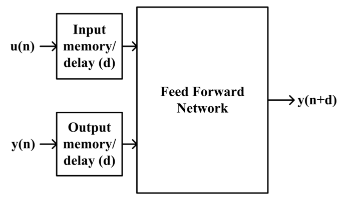

Fig. 11. SP architecture.

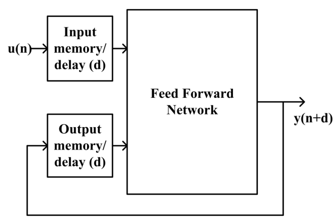

Fig. 12. P architecture.

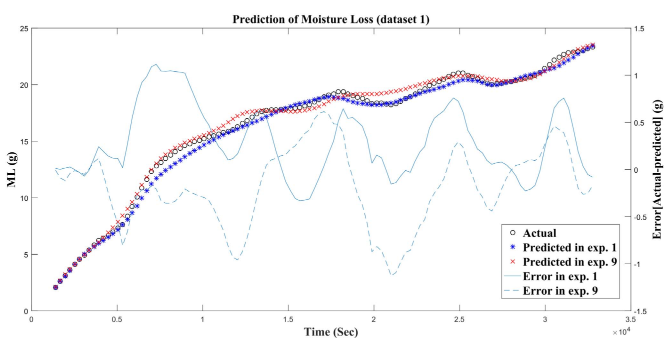

Fig. 13. Actual and predicted MLs along with absolute errors in prediction (Data set 1, Experiments 1 and 9).

For prediction, P architecture is used where estimated output is fed back to the input as shown in Fig. 12 [40].

VI. EXPERIMENTAL METHOD AND RESULT

Fresh tea leaves have been collected from two different gardens. The collected leaves from the first garden are the combination of single leaf and two leaves and a bud whereas leaves collected from the second garden are mostly two leaves and a bud. Withering of tea leaves have been conducted by running the fan at a constant speed after loading the developed rough. The air flow rate has been kept constant at 0.25 m^3/s. The process has been continued at the ambient temperature and RH. Temperature and RH at the inlet and outlet have been recorded by the data acquisition system at intervals of seven seconds. The amount of weight loss of the leaves obtained from the load cell was also recorded by the data acquisition system.

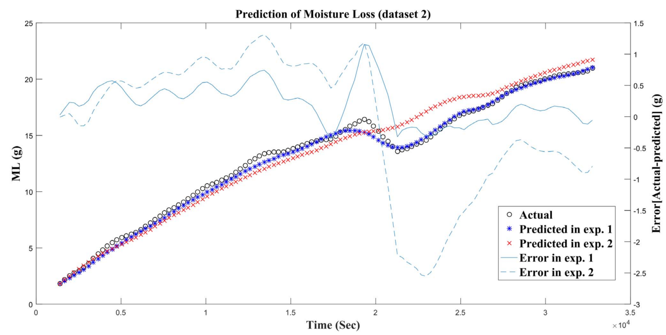

Fig. 14. Actual and predicted ML along with absolute errors in prediction (Data set 2, Experiments 1 and 2).

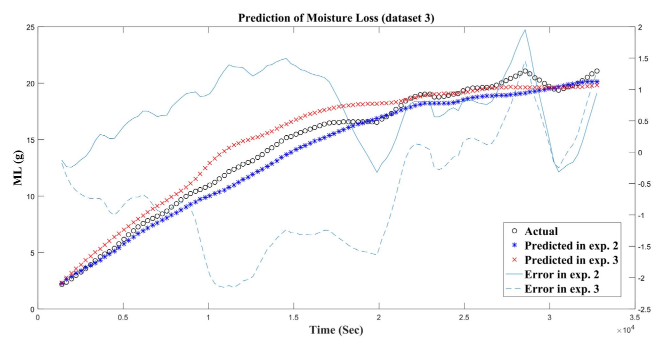

Fig. 15. Actual and predicted ML along with absolute errors in prediction (Data set 3, Experiments 2 and 3).

A total of nine batches of withering have been done out of which four batches have been done for the leaves collected from the first garden and the others from the second garden. The actual ML of the leaves is obtained by the weight loss method in which ML at an instant is obtained by subtracting the weight of the leaves at that instant from its initial weight. A NARX network has been configured to predict ML in withering. The predicted and the actual ML (measured by weight loss method) are compared and analyzed.

A. Data Preparation

The parameters recorded in the process of withering are inlet temperature (T_i), inlet RH (RH_i), outlet temperature (T_o),

This article has been accepted for inclusion in a future issue of this journal. Content is final as presented, with the exception of pagination.

TABLE II
TRAINING PARAMETERS

Experiment No.	Test dataset	Training dataset	Required Time (minutes)	Total no. of iterations	Training Error (g)	Gradient	Regression coefficient (R)
1	1,2	3,4,5,6,7,8,9	30	3543	±0.28	0.000085	0.99996
2	2,3	1,4,5,6,7,8,9	25	2538	±0.19	0.000273	0.99995
3	3,4	1,2,5,6,7,8,9	21	1968	±0.21	0.000023	0.99994
4	4,5	1,2,3,6,7,8,9	24	2140	±0.17	0.000156	0.99996
5	5,6	1,2,3,4,7,8,9	28	2235	±0.16	0.000745	0.99996
6	6,7	1,2,3,4,5,8,9	23	2186	±0.18	0.000453	0.99995
7	7,8	1,2,3,4,5,6,9	20	1864	±0.17	0.000238	0.99996
8	8,9	1,2,3,4,5,6,7	32	3560	±0.24	0.000053	0.99994
9	9,1	2,3,4,5,6,7,8	26	3217	±0.23	0.000294	0.99995

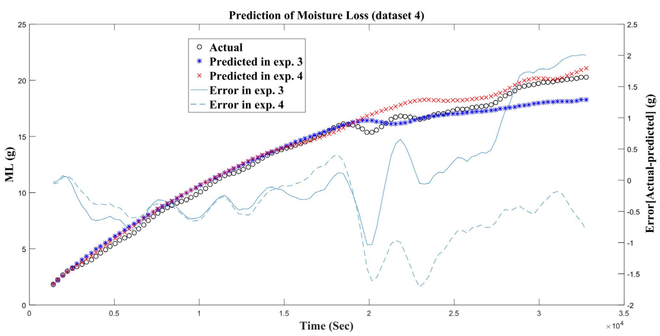

Fig. 16. Actual and predicted ML along with absolute errors in prediction (Data set 4, Experiments 3 and 4).

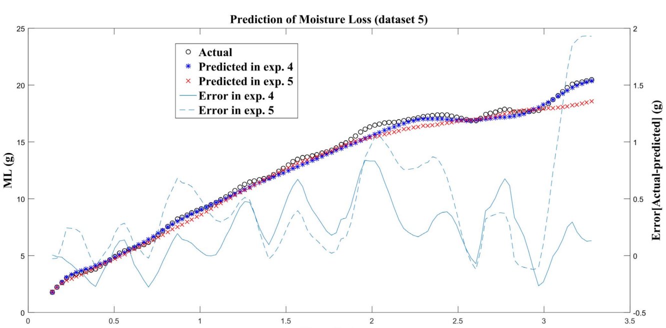

Fig. 17. Actual and predicted ML along with absolute errors in prediction (Data set 5, Experiments 4 and 5).

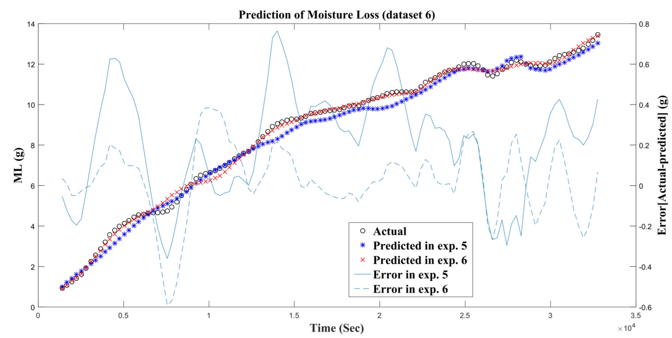

Fig. 18. Actual and predicted ML along with absolute errors in prediction (Data set 6, Experiments 5 and 6).

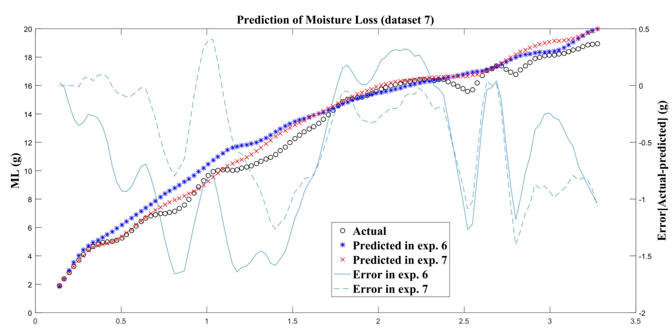

Fig. 19. Actual and predicted ML along with absolute errors in prediction (Data set 7, Experiments 6 and 7).

outlet RH (RH_o), moisture loss (ML), and time (t). To predict ML the parameters used are time (t), inlet temperature (T_i), and the difference of RH (RH_d) which is obtained by subtracting the inlet RH (RH_i) from the outlet RH (RH_o), that is

$$RH_d = RH_o - RH_i. \tag{7}$$

Before using the data sets for training the network, moving average of 256 data points i.e., 1792 s (approximately 30 min) are taken for all the parameters. For training the network, SP architecture (Fig. 11) of NARX network is used. For predicting ML P architecture (Fig. 12) of NARX is used.

B. Configuration of the NARX Network and Training

The NARX network used for training is composed of two layers. The network is configured as shown in Table I. The number of nodes in the hidden layer is chosen in such a way that there is minimum chance of over-fitting and underfitting. Since the input and output of the process are nonnegative and nonlinear, log-sigmoid activation function is used in hidden layer. In the output layer, only one node is used and purely linear (purelin) activation function is used. Levenberg–Marquardt backpropagation is choosen for training, because it is the fastest back propagation algorithm for supervised learning, although it requires more memory space compared to other training algorithms.

This article has been accepted for inclusion in a future issue of this journal. Content is final as presented, with the exception of pagination.

TABLE III
MEAN ERROR WITH RESPECT TO FULL SCALE

Experiment no.	Test dataset	Mean error w.r.t. full scale (%)
1	1	1.24
	2	1.02
2	2	-0.43
	3	3.35
3	3	-3.15
	4	0.57
4	4	2.53
	5	0.99
5	5	2.09
	6	1.58
6	6	0.20
	7	-3.34
7	7	2.37
	8	-0.22
8	8	0.00
	9	-2.44
9	9	-3.60
	1	-0.77

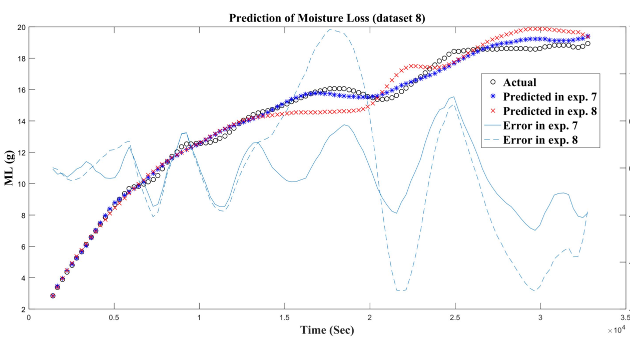

Fig. 20. Actual and predicted ML along with absolute errors in prediction (Data set 8, Experiments 7 and 8).

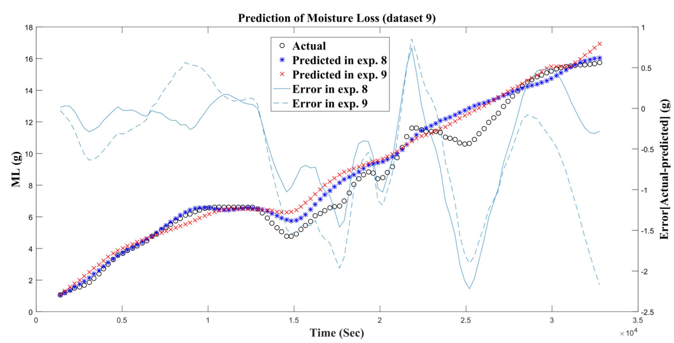

Fig. 21. Actual and predicted ML along with absolute errors in prediction (Data set 9, Experiments 8 and 9).

To train the network, the actual ML measured by the weight loss method is used as the target output. Training of the network is considered to be completed when it achieves the required goal of attaining the set value of the mean-squared error.

C. Prediction of ML

A total of nine experiments has been conducted for predicting ML in withering. In each experiment two data sets of nine have been selected for testing and the remaining seven data sets have been used for training the network. The trained networks have been used to predict the ML in withering. To use the trained NARX network for prediction of ML in withering, it has been changed into a P architecture of NARX network by adding a closed loop i.e., a feedback from predicted output to the input (see Fig. 12). The details of the training parameters are shown in Table II.

Actual and predicted MLs along with absolute errors in prediction for the nine experiments are shown in Figs. 13–21. Each data set has been tested in two different experiments by using different training data set.

The trends of actual MLwith time is nonlinear and the predicted ML follows the trend of actual ML.The mean errors with respect to full scale is given in Table III.

The maximum mean error in prediction is −3.6% (Experiment 9, data set 9). The experiments are conducted in different ambient RH and temperatures. Also the leaf qualities in the experiments are different. Experimental results show that the proposed technique for the prediction of ML works satisfactorily for different ambient conditions and different quality of tea leaves.

VII. Conclusion

Using the developed measurement system, distribution of temperature and RH in the withering trough (prototype) is measured online. The provided network capability of the measurement system implies that the system can be extended to a larger size withering trough used in tea factories which is generally 100 to 120 feet (30 to 36 m) in length and 10 to 15 feet (3 to 5 m) in width. Also, there is a possibility of configuring the nodes as smart sensor. The accuracy of measurements are 1.5 °C for temperature and ±3% for relatiive humidity.

In the reported technique, ML is predicted based on RH and temperature in withering using NARX network. NARX netwok is choosen due to its capability and extensive applicability in predicting nonlinear system output. Since, RH and temperature can be measured online by the developed system; ML can also be predicted online from the information of RH and temperature at the inlet and the outlet of withering trough. For implementing the system in factory no modifications of the existing troughs are required except for installing the sensor modules in the trough. The predicted ML shows a good agreement with actual ML. The maximum mean error in prediction is −3.6% with respect to the full scale.

As in this technique, ML is predicted online, this technique can further be utilized for the control of withering rate to achieve better quality in tea manufacturing. Compared to the other techniques, it has the promising advantages that it requires no representative samples of tea leaves and it can be implemented as the online *in situ* measurement method.

Acknowledgment

The authors would like to thank the Assam Science Technology and Environment Council (ASTEC), Government of Assam and the Department of Science and Technology (DST), Government of India for the use of the facilities created under the projects with sanction numbers ASTEC/S&T/1641(4/1)/2014-14/ 3050 and DST/SSTP/Assam/433, respectively, to conduct the whole experiment. They would also like to thank M. Bhuyan, Research Scholar, from the Department of Electronics and Communication Technology, Gauhati University, Gauhati, India, for his help and support for completing this paper, especially in ANN part, and the management of Barduar Tea Estate and Birjhara Tea Estate for providing the tea leaves to conduct the experiments.

References

[1] J. Liang, H. Yan, P. Puligundla, X. Gao, Y. Zhou, and X. Wan, "Applications of chitosan nanoparticles to enhance absorption and bioavailability of tea polyphenols: A review," *Food Hydrocolloids*, vol. 69, pp. 286–292, Aug. 2017. [Online]. Available: http://dx.doi.org/10.1016/j.foodhyd.2017.01.041

[2] C.-T. Ho, X. Zheng, and S. Li, "Tea aroma formation," *Food Sci. Human Wellness*, vol. 4, pp. 9–27, Mar. 2015. [Online]. Available: http://dx.doi.org/10.1016/j.fshw.2015.04.001

[3] P. Saha, S. Ghorai, B. Tudu, R. Bandyopadhyay, and N. Bhattacharyya, "Feature fusion for prediction of theaflavin and thearubigin in tea using electronic tongue," *IEEE Trans. Instrum. Meas.*, vol. 66, no. 7, pp. 1703–1710, Jul. 2017. [Online]. Available: http://ieeexplore.ieee.org/document/7880645/

[4] P. Sharma *et al.*, "A quartz crystal microbalance sensor for detection of geraniol in black tea," *IEEE Sensors J.*, vol. 15, no. 2, pp. 1178–1185, Feb. 2015. [Online]. Available: http://ieeexplore.ieee.org/stamp/stamp.jsp?arnumber=6906243

[5] Tea Research Association (TRA). *Withering*. Accessed: Jan. 3, 2017. [Online]. Available: http://www.tocklai.net/activities/tea-manufacture/withering/

[6] K. I. Tomlins and A. Mashingaidze, "Influence of withering, including leaf handling, on the manufacturing and quality of black teas—A review," *Food Chem.*, vol. 60, no. 4, pp. 573–580, Dec. 1997, doi: 10.1016/S0308-8146(97)00035-6.

[7] D. Baruah, L. P. Bhuyan, and M. Hazarika, "Impact of moisture loss and temperature on biochemical changes during withering stage of black tea processing on four Tocklai released clones," *Two Bud*, vol. 59, no. 2, pp. 134–142, Jan. 2012. [Online]. Available: http://tocklai.net/wpcontent/uploads/2013/07/TwoBud5922012/Impact%20of%20moisture%20loss%20and%20temperature.pdf

[8] N. T. Omiadze, N. I. Mchedlishvili, J. N. Rodrigez-Lopez, M. O. Abutidze, T. A. Sadunishvili, and N. G. Pruidze, "Biochemical processes at the stage of withering during black tea production," *Appl. Biochem. Microbiol.*, vol. 50, no. 4, pp. 394–397, July. 2014, doi: 10.1134/S0003683814040103.

[9] M. G. Hampton, "Production of black tea," in *Tea: Cultivation to Consumption*, K. C. Wilson and M. N. Clifford, Eds. London, U.K.: Chapman & Hall, 1992, pp. 472–474.

[10] D. Singh, T. Samanta, S. Das, A. K. Ghosh, A. Mitra, and B. C. Ghosh, "Development of a customized trough to study withering of tea leaves," *Two Bud*, vol. 59, no. 2, pp. 143–147, Jan. 2012. [Online]. Available: http://www.tocklai.net/wpcontent/uploads/2013/07/TwoBud5922012/Development%20of%20a%20customized%20trough.pdf

[11] M. Bhuyan, "Measurements in food processing," in *Measurement and Control in Food Processing*. New York, NY, USA: CRC Press, 2007, pp. 125–126.

[12] S. Okamura, Y. Zhang, and N. Tsukamoto, "A new microstripline-type moisture sensor for heavily wet tea leaves," *Meas. Sci. Technol.*, vol. 18, pp. 1022–1028, Feb. 2007, doi: 10.1088/0957-0233/18/4/009.

[13] D. Hazarika, S. Laskar, A. Sarma, and P. K. Sarmah, "PC-based instrumentation system for the detection of moisture content of tea leaves at its final stage," *IEEE Trans. Instrum. Meas.*, vol. 55, no. 5, pp. 1641–1647, Oct. 2006, doi: 10.1109/TIM.2006.881031.

[14] H. M. Ghodake, T. K. Goswami, and A. Chakraverty, "Mathematical modeling of withering characteristics of tea leaves," *Drying Technol.*, vol. 24, no. 2, pp. 159–164, Feb. 2006, doi: 10.1080/07373930600558979.

[15] W. S. Botheju, K. S. P. Amarathunge, and I. S. B. Abeysinghe, "Simulation of trough withering of tea using one dimensional heat and mass transfer finite difference model," *Tropical Agricult. Res.*, vol. 22, no. 3, pp. 282–295, Oct. 2011, doi: http://dx.doi.org/10.4038/tar.v22i3.3701.

[16] A. Chen, H.-Y. Chen, and C. Chen, "Use of temperature and humidity sensors to determine moisture content of oolong tea," *Sensors*, vol. 14, pp. 15593–15609, Aug. 2014, doi: 10.3390/s140815593.

[17] C. J. Geankplis, *Transport Processes and Unit Operations*, 3rd ed. Upper Saddle River, NJ, USA: Prentice-Hall, 1993.

[18] S. A. Kalogirou, "Artificial intelligence in renewable energy applications in buildings," in *Proc. Int. Conf. Integr. Renew. Energy Syst. (RES) Building Struct. CD-ROM*, Patra, Greece, 2005, pp. 112–126. [Online]. Available: http://ktisis.cut.ac.cy/handle/10488/849

[19] H. Chen, J. Zhang, Y. Xu, B. Chen, and K. Zhang, "Performance comparison of artificial neural network and logistic regression model for differentiating lung nodules on CT scans," *Expert Syst. Appl.*, vol. 39, no. 13, pp. 11503–11509, Oct. 2012. [Online]. Available: http://dx.doi.org/10.1016/j.eswa.2012.04.001

[20] H. Bacha and W. Meyer, "A neural network architecture for load forecasting," in *Proc. Int. Joint Conf. Neural Netw.*, Jun. 1992, pp. 442–447. [Online]. Available: http://ieeexplore.ieee.org/document/226948/

[21] C. Cimpoiu, V. M. Cristea, A. Hosu, M. Sandru, and L. Seserman, "Antioxidant activity prediction and classification of some teas using artificial neural networks," *Food Chem.*, vol. 127, pp. 1323–1328, Aug. 2011. [Online]. Available: https://doi.org/10.1016/j.foodchem.2011.01.091

[22] M. J. Barroca, R. P. F. Guiné, A. R. P. Calado, P. M. R. Correia, and M. Mende, "Artificial neural network modelling of the chemical composition of carrots submitted to different pre-drying treatments," *J. Food Meas. Characterization*, Jun. 2017. [Online]. Available: https://link.springer.com/article/10.1007/s11694-017-9563, doi: 10.1007/s11694-017-9563-9.

[23] J. M. P. Menezes, Jr., and G. A. Barreto, "Long-term time series prediction with the NARX network: An empirical evaluation," *Neurocomputing*, vol. 71, pp. 3335–3343, Oct. 2008, doi: 10.1016/j.neucom.2008.01.030.

[24] K. D. V. S. K. Rao, B. I. Rani, and G. Saravana, "Estimation of daily global solar radiation using temperature, relative humidity and seasons with ANN for Indian stations," in *Proc. Int. Conf. Power, Signals, Controls Comput.*, Jan. 2012, pp. 1–6, doi: 10.1109/EPSCICON.2012.6175254.

[25] E. E. Peters, *Fractal Market Analysis: Applying Chaos Theory to Investment and Economics*. Hoboken, NJ, USA: Wiley, 2001.

[26] D. S. G. Pollok, *A Handbook of Time—Series, Signal Processing and Dynamics*. Cambridge, MA, USA: Academic, 1999.

[27] D. P. Mandic and J. A. Chambers. *Recurrent Neural Networks for Prediction: Learning Algorithms, Architectures and Stability*. New York, NY, USA: Wiley, 2001.

[28] T. Lin, B. G. Horne, P. Tino, and C. L. Giles, "Learning long-term dependencies in NARX recurrent neural networks," *IEEE Trans. Neural Netw.*, vol. 7, no. 6, pp. 1329–1351, Nov. 1996, doi: 10.1109/72.548162.

[29] S. Haykin, *Neural Networks*, 2nd ed. London, U.K.: Pearson Education, 1999.

[30] T.-N. Lin, C. L. Giles, B. G. Horne, and S.-Y. Kung, "A delay damage model selection algorithm for NARX neural networks," *IEEE Trans. Signal Process.*, vol. 45, no. 11, pp. 2719–2730, Nov. 1997, doi: 10.1109/78.650098.

[31] *Datasheet of LM35*. Accessed: Jan. 3, 2017. [Online]. Available: http://www.ece.usu.edu/ece_store/spec/lm35dt-3p.pdf

[32] *Datasheet of HIH5030*. Accessed: Jan. 3, 2017. [Online]. Available: https://sensing.honeywell.com/index.php?ci_id=49692

[33] *Datasheet MPC1541*. Accessed: Jan. 3, 2017. [Online]. Available: http://www.microchip.com/downloads/en/DeviceDoc/21653b.pdf

[34] *Datasheet of TLC272*. Accessed: Jan. 3, 2017. [Online]. Available: http://www.ti.com/product/TLC272

[35] *Datasheet of LM336-2.5*. Accessed: Jan. 3, 2017. [Online]. Available: http://www.ti.com/lit/ds/symlink/lm336-2.5-n.pdf

[36] *Datasheet of AD620*. Accessed: Jan. 3, 2017. [Online]. Available: http://www.analog.com/media/en/technical-documentation/data-sheets/AD620.pdf

[37] *Datasheet of Atmega8*. Accessed: Jan. 3, 2017. [Online]. Available: http://www.atmel.com/.../Atmel-8159-8-bit-AVR-microcontroller-ATmega8A_datasheet.pdf

[38] *Atmel Studio4*. Accessed: Jan. 3, 2017. [Online]. Available: http://www.atmel.com›Products›Microcontrollers›AVR8-and32-bitMCUs

[39] S. Chen, S. A. Billings, and P. M. Grant, "Non-linear system identification using neural networks," *Int. J. Control*, vol. 51, no. 6, pp. 1191–1214, Jan. 1990, doi: 10.1080/00207179008934126.

[40] K. S. Narendra and K. Parthasarathy, "Identification and control of dynamical systems using neural networks," *IEEE Trans. Neural Netw.*, vol. 1, no. 1, pp. 4–27, Mar. 1990, doi: 10.1109/72.80202.

[41] MathWorks. *Design Time Series NARX Feedback Neural Networks*. Accessed: Jan. 3, 2017. [Online]. Available: http://in.mathworks.com/help/nnet/ug/design-time-series-narx-feedback-neural-networks.html?searchHighlight=Narx&s_tid=doc_srchtitle

Nipan Das received the M.Sc. degree in instrumentation from Gauhati University, Gauhati, India, in 2009, and the M.Tech degree in electronics design and technology from Tezpur University, Tezpur, India, in 2011.

He is currently a Research Scholar in the Department of Instrumentation and USIC, Gauhati University. His current research interests include embedded system design, signal conditioning and processing, and process instrumentation.

Kunjalata Kalita received the M.Sc. degree in instrumentation from Gauhati University, Gauhati, India, in 2009.

She is a Research Scholar and an Assistant Professor (Contractual) in the Department of Instrumentation and USIC, Gauhati University. Her current research interests include embedded system design, signal conditioning and processing, sensor technology, and wood technology.

P. K. Boruah received the Ph.D. degree from Gauhati University, Gauhati, India, in 1980.

He was a Scientific Officer and a Head with Instruments Division under Forensic Laboratory, Guwahati, Government of Assam, Assam, for a period of 17 years. He also served as a Research and Development Manager, Assam Electronics Development Corporation, Guahati, for a period of 3 years. He retired as a Professor from the Department of Instrumentation and USIC, Gauhati University, in 2012. His current research interests include experimental cosmic ray physics, detectors and instrumentation, and signal processing and development of smart transducer instrumentation and sensor networks.

Utpal Sarma (M'14) received the M.Sc. degree in physics and the Ph.D. degree from Gauhati University, Gauhati, India, in 1998 and 2010, respectively.

In 1999, he joined the Department of Physics, B. Borooah College, Guwahati, as a Lecturer. He joined Gauhati University, as an Assistant Professor, in 2007, where he is currently an Associate Professor. His current research interests include embedded system for agro industries, sensor instrumentation, and microenergy harvesting devices.